IEEE Access
Multidisciplinary | Rapid Review | Open Access Journal

Received August 8, 2019, accepted August 21, 2019, date of publication August 29, 2019, date of current version September 13, 2019.

Digital Object Identifier 10.1109/ACCESS.2019.2938331

Sum-Throughput Maximization by Power Allocation in WBAN With Relay Cooperation

SHUANG LI[1], FENGYE HU[1], (Member, IEEE), ZHI MAO[1], ZHUANG LING[1], AND YONGKUI ZOU[2]

[1]College of Communication Engineering, Jilin University, Changchun 130025, China
[2]College of Mathematics, Jilin University, Changchun 130025, China

Corresponding author: Fengye Hu (hufy@jlu.edu.cn)

This work was supported in part by the Jilin Provincial Science and Technology Department Key Scientific and Technological Project under Grant 20190302031GX, in part by the Changchun Scientific and Technological Innovation Double Ten Project under Grant 18SS010, in part by the National Natural Science Foundation of China under Grant 61671219 and Grant 11771179, and in part by the Jilin Province Development and Reform Commission Project under Grant 2017C046-3.

ABSTRACT In this paper, we investigate an energy harvesting wireless body area network (WBAN) with relay cooperation, where the destination nodes and the relay simultaneously harvest energy from the radio frequency (RF) source, then the destination nodes transmit data to the source by maximum ratio combining (MRC) transmission mode. We study the optimal design for relay power splitting ratio in each relaying sub-slot and the destination nodes power allocation to maximize the sum-throughput with the proposed protocol. The optimization problem is divided into two cases, destination node power limit (DPL) case and relay power limit (RPL) case. In essence, the problem is a joint-objective optimization and is solved by the Lagrangian multiplier method. Simulation results show that our proposed optimal method can greatly improve the sum-throughput compared with conventional mean power allocation (MPA) method and mean time allocation (MTA) method. Moreover, a significant sum-throughput promotion is achieved on the RPL case over the DPL case.

INDEX TERMS Relay cooperation, energy harvesting nodes, optimal power allocation protocol, sum-throughput, WBAN.

I. INTRODUCTION

In recent years, the reach for wireless body area network (WBAN) has experienced unprecedented growth [1]. WBAN is a real-time communication system in which a variety of sensor nodes are placed in, on, or around the human body [2]. The application of WBAN for medical treatment such as health care, bodily vital statistics detection and disease prevention is driven both by consumers and industry [3]–[5]. In traditional WBAN, the network is limited by the requirement for a battery. The sensor nodes are powered by batteries, which increases the difficulty for changing the battery, such as sensor nodes implanted in the body [6], [7]. Considering the human health, low-power operation pays an important role in WBAN [8]. And reliable communication, low power consumption and long life time are the most important techniques required by WBAN.

Recently, energy harvesting (EH) for powering on/in-body sensor nodes is a significant technology to provide a promising solution, which can break the battery limitation. The sensor nodes have potential for EH include mechanical, thermal, natural and radio frequency (RF) [9]–[11]. In cooperative WBAN, it is necessary to use EH technology because of the EH constraints at relay [12], [13]. In [14], the authors discussed a practical receiver architecture, where the circuits for harvesting energy from signals directly are operated in a time switching (TS) or power splitting (PS) manner. In [15], two types of relaying protocols, named TS protocol and PS protocol, are proposed in amplify-and-forward (AF) relaying network. In order to achieve various trade-offs between the maximum ergodic capacity and the maximum average harvested energy, the authors derive the PS rule at the receiver

The associate editor coordinating the review of this article and approving it for publication was Xiaodong Yang.

and investigate the effect [16]. Cooperative communication can increase the transmission diversity gain and maintain reliability [17], [18]. In [19], the cooperative network with maximum ratio combining (MRC) has been considered compared with direct transmission (DT) and relay transmission (RT), which reduces the outage probability in wireless cooperative network. However, these studies aim at a single-user wireless powered communication network (WPCN), which can not represent practical networks.

EH in muti-user wireless network has been introduced. A two-user wireless coopreative network is considered [20]–[22]. In [20], the authors study the cooperation between two users by use of energy efficient network coding technique, which provides superior performance compared to non-cooperative communication. Reference [21] maximizes the weighted sum-rate of the two users by jointly optimizing the time and power allocation to achieve more balanced throughput. Without a help relay, there exists interference in [20], [21]. Reference [22] proposes an iterative power allocation algoruthm based on decode-and-forward (DF) with mutli-antenna relaying network, and shows that this model can not noly raise the channel capacity, but also improve the detection probability.

A recent work in [23] has discussed the optimal sum-throughput by PS and TS with multi-user network, but which does not consider system capacity limit. Reference [24] extended [23] and considered the limitation of energy causality. It optimized each user power with the aim of sum-throughput, and solved it by Lambert W-Function method. [25] investigated a cooperative network with multiple users and relays, and studied the the optimal design for PS ratio at each relay. The effect of power allocation on tradeoff between the achievable throughput and harvested energy is characterized in [26]. But all the discussion in [23]–[26] do not mention that the destination nodes and the relay simultaneously harvest energy, and how to jointly optimize the power allocation at destination multiple nodes and a relay.

In this paper, we focus on a cooperative WBAN with a relay, where the destination nodes and the relay simultaneously harvest energy broadcasted by the source, then the destination nodes transmit data to the source through cooperation. A similar system model for multi-point WBAN with harvesting energy has been investigated in [27], where the cooperative transmission is not taken into account. Since WBAN is a short-distance and high-dynamic communication network, the combination of direct link and relaying transmission is reasonable. Previous works are mainly based on the assumptions made on relay about the EH process [28], which ignores the power allocation of sensor nodes. According to the energy limitation, such as [24], we consider the power limition of both the destination nodes and relay. In addition, we will significantly discuss the allocation of harvested energy at relay among all relaying sub-slots, which is the different from existing works. The main contributions of this paper are summarized as follows:

- We perform a comprehensive study on optimal power allocation on MRC (OPA-MRC) protocol for a relaying network by taking into account PS at each sensor node, relay power allocation among all relaying sub-slots as well as the limitation of energy causality.
- With the proposed protocol, we formulate the sum-throughput optimization problem as a joint-objective linear programming problem. In order to maximize the sum-throughput, the optimal problems are solved by the Lagrangian multiplier method. And we derive the solution for the optimal power allocation ratio at each destination node and relay.
- Compared with the traditional mean allocation schemes and OPA-MRC scheme on the sum-throughput in WBAN, the performance of the OPA-MRC protocol always attains the best sum-throughput. Then, we evaluate performance of the sum-throughput under various system parameter settings.

The remainder of this paper is organized as follows. In Section II, we describe the system model. Section III prensents the OPA-MRC protocol. In Section IV, a joint-objective programming solution for the optimal design for power allocation is proposed in two cases. Numerical results are presented in Section V. Finally, we conclude this paper in Section VI.

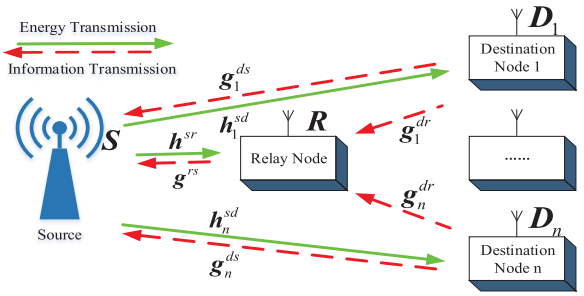

FIGURE 1. System model.

II. SYSTEM MODEL

In Fig.1, an energy harvesting cooperative communication model in WBAN is considered, which features one RF source (S), one cooperative relay (R) and n on/in-body destination nodes denoted by D_i, $i = 1, 2, \cdots, n$. D_i and R can harvest energy by the source broadcasting RF signals, which is stored in the battery. Besides, D_i transmits the information data to S and R. We assume that h^{sr} and g^{rs} denote the channel coefficients of $S - R$ and $R - S$, as well as h_i^{sd} and g_i^{ds} denote the channel coefficients of $S - D_i$ and $D_i - S$. Let g_i^{dr} be the channel coefficent of $D_i - R$. The distance of $S - R$ is expressed as d_0, the distance of $S - D_i$ is expressed as d_i, $i = 1, 2, \cdots, n$. In this system model, all nodes in half-duplex mode are equipped with a single antenna.

For our propagation model, the communication channels are independent and conform to the WBAN channel path loss model. In this paper, the channel model is

$$PL(d_i) = PL' + 10\phi \log_{10}(\frac{d_i}{d'}) \quad (1)$$

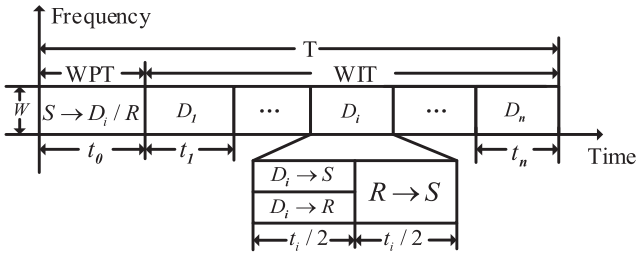

FIGURE 2. Transmission protocol.

where ϕ implies path loss index, d' implies the reference distance, and PL' is path loss at a distance of d' from the reference distance.

III. TRANSMISSION PROTOCOL

In order to prevent wireless interference, all nodes in the system model work on the time-division-multiple-access (TDMA), in which only one node can transmit at any given time slot. So the transmission based on OPA-MRC protocol is shown in Fig.2, where the total transmission time T is divided into $(1+n)$ time slots with duration of $T/(1+n)$. In addition, the whole communition process is divided into two phases, wireless powered transmission (WPT) and wireless information transmission (WIT). In the WPT phase, the amount of time slot t_0 is allocated to D_i and R to harvest energy from S. In the WIT phase, the time slot t_i is allocated to D_i to transmit data back to S. The half of t_i is used for the information transmission from D_i to R and S simultaneously. The remaining half of t_i is used for R to transmit information towards S. Moreover, we adopt DF relaying mode in this work. The relevant formula is analyzed as follows.

A. WPT PHASE

In the WPT phase of duration t_0, the source broadcasts RF signals to D_i and R. Hence, the received signal at D_i can be expressed as

$$y_i^d = \sqrt{P_s} h_i^{sd} x_s + n_i \tag{2}$$

where P_S represents the transmit power of S and h_i^{sd} represents the channel coefficient $S-D_i$. The transmitted baseband signal of S with unit power is denoted by x_s. And n_i is the antenna noise.

Therefore, we get the harvested energy at D_i is given by

$$E_i^d = \eta t_0 P_s \left| h_i^{sd} \right|^2 = \frac{\eta P_s \left| h_i^{sd} \right|^2 T}{1+n} \tag{3}$$

where η $(0 < \eta \leqslant 1)$ is the energy harvesting conversion efficiency at each node.

Meanwhile, the received signal at the relay can be obtained as

$$y^r = \sqrt{P_s} h^{sr} x_s + n_r \tag{4}$$

where h^{sr} is the channel coefficient from $S - R$ and n_r is the zero mean additive white Gaussian noise (AWGN) at R.

In addition, the amount of energy harvested by the relay is expressed as

$$E^r = \eta t_0 P_s \left| h^{sr} \right|^2 = \frac{\eta P_s \left| h^{sr} \right|^2 T}{1+n} \tag{5}$$

B. WIT PHASE

In the WIT phase, D_i transmit independent information data to S in their allocated time slots t_i with a cooperative relay, which includes three part, direct transmission part, relay transmission part and MRC transmission part.

1) DIRECT TRANSMISSION PART

In the direct transmission part, the source receives the data from D_i in the first half of t_i. And we give the transmit power of D_i from (3) as

$$P_i^d = \frac{2E_i^d}{t_i} \rho_i^d = 2\eta P_s \left| h_i^{sd} \right|^2 \rho_i^d \tag{6}$$

where ρ_i^d $\left(0 < \rho_i^d \leqslant 1\right)$ is the power splitting ratio at each destination node. So the received signal at S can be given by

$$y_i^s = \sqrt{P_i^d} g_i^{ds} x_i + n_s \tag{7}$$

where g_i^{ds} is the channel coefficient $D_i - S$ and x_i is the transmitted baseband signal of D_i with unit power. n_s denotes the noise at S. From (6) and (7), the signal noise ratio (SNR) at S for each destination node can be presented as

$$\gamma_i^d = \frac{P_i^d \left| g_i^{ds} \right|^2}{\sigma_s^2} = \frac{2\eta P_s \left| h_i^{sd} \right|^2 \left| g_i^{ds} \right|^2}{\sigma_s^2} \rho_i^d \tag{8}$$

where σ_s^2 is the received noise power at the source.

2) RELAY TRANSMISSION PART

In the relaying transmission part, the first stage is the signal transmission from D_i to R at the same time with the direct transmission in the first half of t_i. The received signal at R is given by

$$y_i^{r1} = \sqrt{P_i^d} g_i^{dr} x_i + n_r \tag{9}$$

where g_i^{dr} is the channel coefficient $D_i - R$. Substituting the (6) into (9), the SNR at R can be represented as

$$\gamma_i^{r1} = \frac{P_i^d \left| g_i^{dr} \right|^2}{\sigma_r^2} = \frac{2\eta P_s \left| h_i^{sd} \right|^2 \left| g_i^{dr} \right|^2}{\sigma_r^2} \rho_i^d \tag{10}$$

Next, the relay uses part of the harvested energy for information transmission in the second half of t_i. Form (5), we give the transmit power of R as

$$P_i^r = \frac{2E^r}{t_i} \rho_i^r = 2\eta P_s \left| h^{sr} \right|^2 \rho_i^r \tag{11}$$

where ρ_i^r $(0 < \rho_i^r \leqslant 1)$ is the power splitting ratio at the relay in the ith relaying sub-slot. Therefore, the received signal at the source is presented as

$$y_i^{r2} = \sqrt{P_i^r} g^{rs} x_r + n_s \tag{12}$$

where g^{rs} is the channel coefficient between R and S, and x_r is a unit-power of the relay. With the previous analysis, we obtain SNR of the $R-S$ link as

$$\gamma_i^{r2} = \frac{P_i^r |g^{rs}|^2}{\sigma_s^2} = \frac{2\eta P_s |h^{sr}|^2 |g^{rs}|^2}{\sigma_s^2}\rho_i^r \tag{13}$$

3) MRC TRANSMISSION PART

At the end of the relaying transmission, MRC of the direct and the relay transmission is applied at S. Obviously, the achievable SNR at the source for ensuring the success of decoding information in the whole transimission part should satisfy

$$\gamma_i^{MRC} = \min(\gamma_i^{r1}, \gamma_i^d + \gamma_i^{r2}) \tag{14}$$

The function of a random variable of the form in (14) has been extensively studied in [22], [25]. The first term in (14) represents the maximum SNR at which the relay can successfully decode the destination information, while the second term in (14) represents the maximum SNR at which the source can reliably decode the destination information given repeated transmissions from the destination node and source. Thus, we get the sum-throughput for the whole system as

$$\begin{aligned} R_i^{MRC} &= \frac{1}{2(1+n)}\log_2(1+\gamma_i^{MRC}) \\ &= \begin{cases} \frac{1}{2(1+n)}\log_2(1+\gamma_i^{r1}), & \gamma_i^{r1} \leqslant \gamma_i^d + \gamma_i^{r2} \\ \frac{1}{2(1+n)}\log_2(1+\gamma_i^d+\gamma_i^{r2}), & \gamma_i^{r1} > \gamma_i^d + \gamma_i^{r2} \end{cases} \end{aligned} \tag{15}$$

where $\rho^d = [\rho_1^d, \rho_2^d, ...\rho_n^d]$ and $\rho^r = [\rho_1^r, \rho_2^r, ...\rho_n^r]$.

IV. OPTIMIZATION STRATEGY

In this section, we will study an energy harvesting in cooperative relaying WBAN based on OPA-MRC transmission protocol described in Section III, where the destination nodes and relay all are confined system. Specifically, we aim to maximize the information sum-throughput for the whole system. Hence, the maximization problem through the joint-objective programming can be described as

$$\begin{aligned} (P1): \max_{\rho^d,\rho^r} \ & \sum_{i=1}^{n} R_i^{MRC} \\ s.t. \quad C1 \quad & \rho_i^d \geqslant 0, \rho_i^r \geqslant 0 \\ C2 \quad & \frac{\eta P_s |h_i^{sd}|^2 T}{1+n}\rho_i^d \leqslant E_i^d \\ C3 \quad & \sum_{i=1}^{n} \frac{\eta P_s |h^{sr}|^2 T}{1+n}\rho_i^r \leqslant E^r \\ C4 \quad & \sum_{i=1}^{n}\left[\frac{2E^r}{t_i}\rho_i^r + \frac{4E_i^d}{t_i}\rho_i^d\right] \leqslant P_0 \end{aligned} \tag{16}$$

Note that $C1$ includes the non-negative constraints on ρ_i^d and ρ_i^r. $C2$ and $C3$ are the limition of harvested energy causality at D_i and R, which should be less than the maximum harvested energy in WPT phase. By introducing new variables in P_0 which is a fixed value and less than P_s, $C4$ presents the total power used for transmission at the relay and destination nodes are restricted.

Lemma 1: When $\gamma_i^{r1} = \gamma_i^d + \gamma_i^{r2}$, γ_i^{MRC} has the maximum in point-to-point WBAN.

Proof: Please refer to [29] and Fig.3.

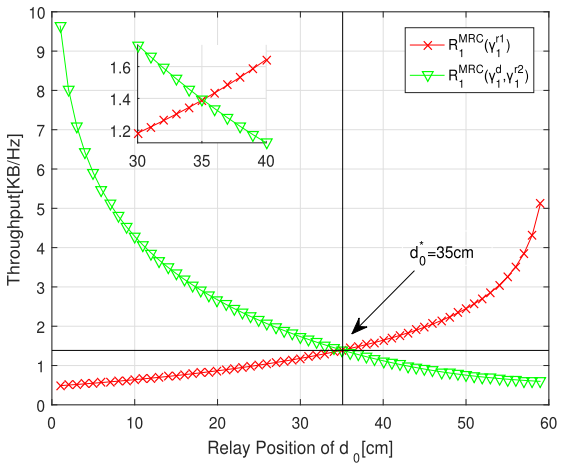

FIGURE 3. Throughput versus in a point-to-point WBAN.

In Fig.3, the throughput is shown in (14) with $n = 1$, $d_1 = 60cm$, and $t_0 = 0.5$. It is oberserved that the maximum throughput is procurable on the intersection of two curves. It is also oberserved that the throughput improves with d_0 increasing when $d_0 < d_0^* = 35cm$ and $R_1^{MRC} = \frac{1}{2(1+n)}\log_2(1+\gamma_1^{r1})$, but deteriorates when $d_0 > d_0^*$ and $R_1^{MRC} = \frac{1}{2(1+n)}\log_2(1+\gamma_1^d+\gamma_1^{r2})$. Hence, when $\gamma_i^{r1} = \gamma_i^d + \gamma_i^{r2}$, γ_i^{MRC} gets the maximum value, the sum-throughput of (P1) has the maximum. For simplicity, the paper assumes $\sigma_s^2 = \sigma_r^2 = \sigma^2$. The optimal power distribution condition for the relay and each node is given by

$$\frac{\rho_i^r}{\rho_i^d} = \frac{\left(|g_i^{dr}|^2 - |g_i^{ds}|^2\right)E_i^d}{|g^{rs}|^2 E^r} \tag{17}$$

In our system, because of the limition of harvested energy causality at D_i and R, there are two cases in the optimization problem: one case is the destination node power limit (DPL), when $\sum_{i=1}^{n}\frac{\left(|g_i^{dr}|^2-|g_i^{ds}|^2\right)E_i^d}{|g^{rs}|^2} < E^r$; the other one is the relay power limit (RPL), when $\sum_{i=1}^{n}\frac{\left(|g_i^{dr}|^2-|g_i^{ds}|^2\right)E_i^d}{|g^{rs}|^2} \geqslant E^r$.

A. DPL CASE

Introduting a new variables G_i^{DPL}, the (17) can be reformulated as

$$G_i^{DPL} = g_i E_i \tag{18}$$

where G_i^{DPL} is the product of g_i and E_i. In (18), it is assumed that $g_i = \frac{|g_i^{dr}|^2-|g_i^{ds}|^2}{|g^{rs}|^2}$, and E_i is the ratio of E_i^d and E^r.

Then we obtain the transmit power ratio at the relay as

$$\rho_i^r = G_i^{DPL}\rho_i^d \tag{19}$$

Substituting the (19) into ($P1$), it is changed by simplifying as

$$\begin{aligned}(P2):\ \max_{\boldsymbol{\rho}^d}\ & \sum_{i=1}^{n} R_i^{MRC} \\ s.t.\quad & C1\quad \rho_i^d \geqslant 0 \\ & C2\quad \rho_i^d \leqslant 1 \\ & C3\quad \sum_{i=1}^{n} G_i^{DPL}\rho_i^d \leqslant 1 \\ & C4\quad \sum_{i=1}^{n}(2E_i^d + G_i^{DPL}E^r)\frac{2T}{t_i}\rho_i^d \leqslant P_0 \end{aligned} \tag{20}$$

In (20), the constrant $C1$ is the non-negative constraints on ρ_i^d. $C2$ shows the value range of ρ_i^d, and $C3$ represents the sum of allocated power ratio at relay ρ_i^r in all n relaying sub-slots.

Lemma 2: $\sum_{i=1}^{n} R_i^{MRC}$ is a convex function of $\boldsymbol{\rho}^d$ for any given $i \in \{1, ..., n\}$.

Proof: Please refer to Appendix A.

Compared to the sum of the harvested energy at the relay and destination nodes with P_0, the system power should satisfy

$$P = \min\left\{\frac{2T}{1+n}(\sum_{i=1}^{n} E_i^d + E^r),\ P_0\right\} \tag{21}$$

In (21), P denotes maximum system power. The first term in (21) represents the harvested total energy at all nodes. Requiring the system to meet the limition of energy causality results in the minimum of the two power in (21). As a result, the optimal allocation problem of the destination nodes can be formulated as

$$\begin{aligned}(P3):\ \max_{\boldsymbol{\rho}^d}\ & \sum_{i=1}^{n} R_i^{MRC} \\ s.t.\ & C1\ \rho_i^d \geqslant 0 \\ & C2\ \rho_i^d \leqslant 1 \\ & C3\ \sum_{i=1}^{n}(2E_i^d + G_i^{DPL}E^r)\frac{2T}{t_i}\rho_i^d \leqslant P \end{aligned} \tag{22}$$

As described above, the constrants $C1$, $C2$ and $C3$ are linear inequalities of ρ_i^d. From Lemma 2, the objective function is convex of ρ_i^d. Therefore, ($P3$) is a convex optimization problem and can be solved by convex optimization techniques and tools. The corresponding Lagrangian function is calculated by (23), as shown at the bottom of this page. The λ_i, μ_i and α are the Lagrangian multiplier vectors associated with $C1$, $C2$ and $C3$ in (22). In addition, we give the Lagrangian multiplier initial values, then through iteration the primal variables are found using Karush-Kuhn-Tucker (KKT) conditions for the given multipliers. So the sub-gradient method is used to update the multiplier in the optimization problem. The first order necessary condition is

$$\frac{\partial L_1}{\partial \rho_i^d}|_{\rho_i^d=\rho_i^{d*}} = 0 \tag{24}$$

The optimum solution of ρ_i^d can be written as (25), as shown at the bottom of this page.

To solve the optimization problem, sub-gradient method is used to update the Lagrangian multipliers. The specific updating algorithm is obtained as follows:

$$\begin{aligned}\lambda_i^{t+1} &= \left[\lambda_i^t - a_i^t\rho_i^d\right] \\ \mu_i^{t+1} &= \left[\mu_i^t - b^t\left(1-\rho_i^d\right)\right] \\ \alpha^{t+1} &= \left[\alpha^t - c^t\left(P - \frac{2T}{t_i}\sum_{i=1}^{n}\left(2E_i^d + G_i^{DPL}E^r\right)\rho_i^d\right)\right] \end{aligned} \tag{26}$$

where t is the iterative times, and a_i^t, b_i^t, c^t are iteration step sizes.

B. RPL CASE

Introduting a new variables $J_i^{RPL} = \frac{1}{g_i E_i}$, so the transmit power ratio at each destination node is written as

$$\rho_i^d = J_i^{RPL}\rho_i^r \tag{27}$$

Substituting the (27) into ($P3$), it is changed as

$$\begin{aligned}(P4):\ \max_{\boldsymbol{\rho}^r}\ & \sum_{i=1}^{n} R_i^{MRC} \\ s.t.\quad & C1\ \rho_i^r \geqslant 0 \\ & C2\ \sum_{i=1}^{n}\rho_i^r \leqslant 1 \\ & C3\ \sum_{i=1}^{n}(2J_i^{RPL}E_i^d + E^r)\frac{2T}{t_i}\rho_i^r \leqslant P \end{aligned} \tag{28}$$

$$L_1(\rho_i^d, \lambda_i, \mu_i, \alpha) = \frac{1}{2(1+n)}\sum_{i=1}^{n}\log_2\left[1 + 2(1+n)E_i^d\frac{\left|g_i^{dr}\right|^2\rho_i^d}{\sigma^2}\right] - \lambda_i\rho_i^d + \mu_i(1-\rho_i^d) + \alpha\left[P - 2(1+n)\sum_{i=1}^{n}\left(2E_i^d + G_i^{DPL}E^r\right)\rho_i^d\right] \tag{23}$$

$$\rho_i^{d*} = \left[\frac{2(1+n)E_i^d\left|g_i^{dr}\right|^2}{2ln2(1+n)\left[\lambda_i + \mu_i + \alpha\left(2E_i^d + G_i^{DPL}E^r\right)\right]\sigma^2} - 1\right] / \left[2(1+n)E_i^d\frac{\left|g_i^{dr}\right|^2}{\sigma^2}\right] \tag{25}$$

Lemma 3: $\sum_{i=1}^{n} R_i^{MRC}$ is a convex function of $\boldsymbol{\rho}^r$ for any given $i \in \{1, ..., n\}$.

Proof: Please refer to Appendix B.

As metioned above, the constrants $C1$, $C2$ and $C3$ are linear inequalities of ρ_i^r. From Lemma 3, the objective function is convex of ρ_i^r. Similarly, ($P4$) also can be solved through lagrangian multiplier method and KKT conditions. The corresponding Lagrangian function is derived by (29), as shown at the bottom of this page, grangian multiolier vectors. The first order condition of ($P4$) is

$$\frac{\partial L_2}{\partial \rho_i^r}|_{\rho_i^r=\rho_i^{r*}} = 0 \tag{30}$$

The optimum solution of ρ_i^r can be written as (31), as shown at the bottom of this page. The υ_i, θ and ξ are the Lagrangian multiolier vectors associated with $C1$, $C2$ and $C3$ in (28). The specific updating algorithm can be obtained as follows:

$$\begin{aligned}
\upsilon_i^{t+1} &= \left[\upsilon_i^t - d^t \rho_i^r\right] \\
\theta^{t+1} &= \left[\theta^t - e^t\left(1 - \sum_{i=1}^{n} \rho_i^r\right)\right] \\
\xi^{t+1} &= \left[\xi^t - f^t\left(P - \frac{2T}{t_i}\sum_{i=1}^{n}(2J_i^{RPL}E_i^d + E^r)\rho_i^r\right)\right]
\end{aligned} \tag{32}$$

where d^t, e^t, f^t are iteration step sizes.

To summarize, the iteration step size is positive and steadily decreases. When the value between two successive the objective function is mostly same, the algorithm converges [32]. In addition, one algorithm to solve (P3) is given in Algorithm 1. And the algorithm of (P4) is same as that of (P3), which are not presented here due to space limitation.

V. SIMULATION RESULTS

In this section, we give numerical results to demonstrate our analysis and proposal presented algorithms in Section IV. Meanwhile, the impact of various important system parameters is discussed for the performance of the cooperative relaying WBAN. In our simulations, we assume the transmit power at S, $P_s = 1mw$, and the energy harvesting efficiency $\eta = 0.85$. Due to the low transmission power of the body environment, the noise power and the system power limit should be small enough, so they are set as $\sigma_s^2 = \sigma_r^2 = \sigma^2 = -134\ dBm$ and $P_0 = -45\ dBm$.

Algorithm 1 Algorithm To Slove (P3)

Initialize λ_i, μ_i, α.
Set $t = 0$.
repeat
1. According to given system parameters, compute ρ_i^{d*} using (25).
2. Update λ_i, μ_i, α using the sub-gradient given by (26).
3. If the stopping criteria of the sub-gradient method is not met, $t = t + 1$.

until
$|\lambda_i^{t+1} - \lambda_i^t| < \delta$ or $|\mu_i^{t+1} - \mu_i^t| < \delta$ or $|\alpha^{t+1} - \alpha^t| < \delta$ or $t > t_m$, where $\delta > 0$ is a given error tolerance and t_m is the maximum iterate times.

TABLE 1. Simulation parameters of WBAN.

parameter	arm	torso	arm+torso
PL'	32.2	41.2	35.7
d'	10	10	10
ϕ	3.35	3.23	3.38

With the sum-throughput achieved by the direct link, it can enhance the system performance in relaying network [30]. So we set $n = 2$, and S, R and D_i are all place in a straight line. Every destination node is independent of each other. The distance of d_1 is 55cm and the distance d_2 is 60cm. From (1), we can get the channel gain, which are $10^{-\frac{PL(d_i)}{10}}$. The parameter values of this model are shown in Table 1 [31].

A. EFFECT OF RELAY POSITION

In Fig.4, we give the impact of the different distance between S and R on the sum-throughput. For comparison, we also plot the performance of mean power allocation on MRC (MPA-MRC), mean power allocation based based on RT (MPA-RT) and mean time allocation based on DT (MTA-DT) protocols. It is illustrated that there exists a unique d_0^* which gives the best throughput expect DT. As d_0 increases, when $d_0 \leqslant d_0^*$, the throughput improves because the channel gain of $R-D_i$ gets better, but the system is limited by each destination node transmission power; when $d_0 > d_0^*$, the throughput deteriorates because the energy harvested at R reduces and the system is limited by relay power. The coincidence curves show that the sum-throughput is same on the DPL case for three schemes expect DT. It is noteworthy that OPA-MRC

$$\begin{aligned}
L_2(\rho_i^r, \upsilon_i, \theta, \xi) = \frac{1}{2(1+n)}\sum_{i=1}^{n}\log_2\left[1 + 2(1+n)\left(\frac{E^r\left|g_i^{rs}\right|^2 + J_i^{RPL}E_i^d\left|g_i^{ds}\right|^2}{\sigma^2}\right)\rho_i^r\right] - \upsilon_i\rho_i^r \\
+ \theta(1 - \textstyle\sum_{i=1}^{n}\rho_i^r) + \xi\left[P - 2(1+n)\sum_{i=1}^{n}\left(2J_i^{RPL}E_i^d + E^r\right)\rho_i^r\right]
\end{aligned} \tag{29}$$

$$\rho_i^{r*} = \left[\frac{\frac{2(1+n)}{\sigma^2}\left(E^r\left|g^{rs}\right|^2 + J_i^{RPL}E_i^d\left|g_i^{ds}\right|^2\right)}{2ln2(1+n)\left[\upsilon_i + \theta + \xi\left(2J_i^{RPL}E_i^r + E^r\right)\right]} - 1\right] / \left[\frac{2(1+n)}{\sigma^2}\left(E^r\left|g^{rs}\right|^2 + J_i^{RPL}E_i^d\left|g_i^{ds}\right|^2\right)\right] \tag{31}$$

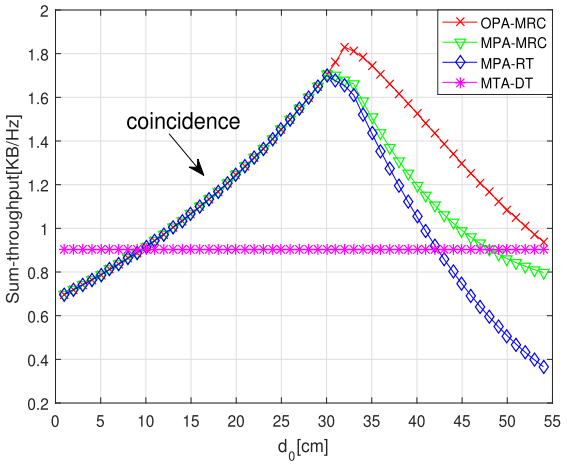

FIGURE 4. Optimal sum-throughput in different distance between source and relay D_0.

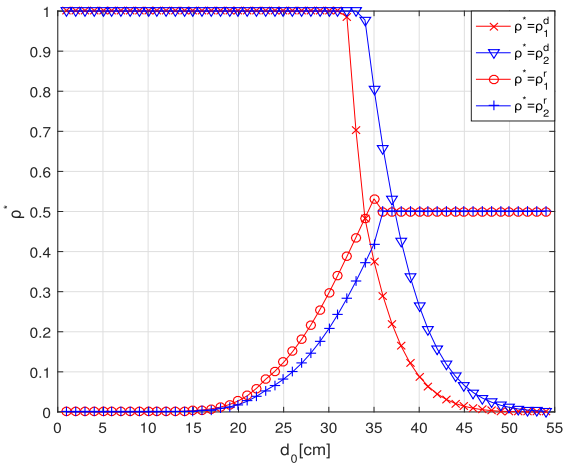

FIGURE 5. Optimal power splitting at destination nodes ρ_i^{d*} and relay ρ_i^{r*} on OPA-MRC protocol.

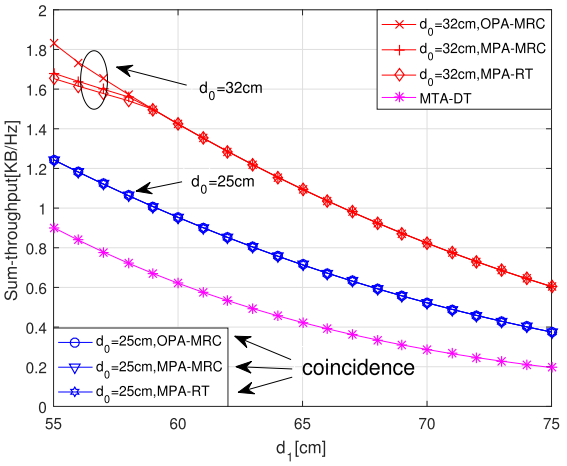

FIGURE 6. Optimal sum-throughput in different distance between source and destination node d_1 on the DPL case.

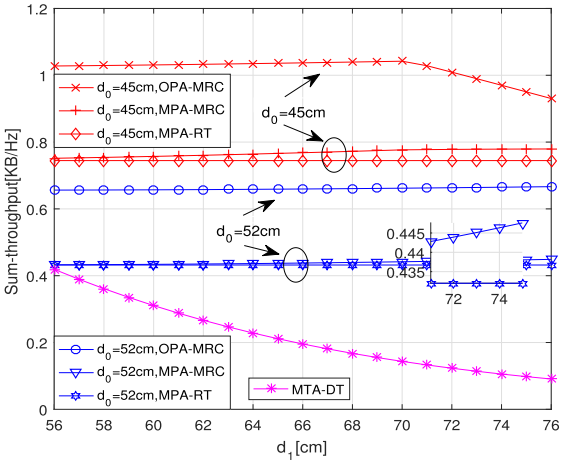

FIGURE 7. Optimal sum-throughput in different distance between source and destination node d_1 on the RPL case.

scheme always has the best sum-throughput, while other three schemes are inferior, and as d_0 increases, the performance gap becomes more pronounced.

The best power splitting ratio of D_i and R based on OPA-MRC protocol for different relay positions are depicted in Fig.5. We see that with the increase of d_0, the value of ρ_i^{d*} remains stable at the maximum then declines gradually, while the value of ρ_i^{r*} stably uprises then hovers at 0.5. It is proved that the system is limited in destination node power when meets $\sum_{i=1}^{n} \frac{|g_i^{dr}|^2 - |g_i^{ds}|^2}{|g^{rs}|^2} E_i^d < E^r$, otherwise limited in relay power.

B. EFFECT OF DESTINATION NODE POSITION

Fig.6 and Fig.7 depict the impact of destination node position on the sum-throughput in different cases, DPL case and RPL case, separately. In order to better compare the effect of different key parameters, we also exhibit the performance with $d_0 = 25cm$ and $d_0 = 32cm$ in Fig.6. As d_1 increases, the sum-throughput of direct link and the cooperative scheme all decline, but the OPA-MRC protocol always attains the best throughput among all four proposed protocols. This observation indicates that, a large d_1 implies farther distance of $R - D_i$ and $S - D_i$, which signifies that the less energy is harvested at D_i and the smaller channel gain is available, so the sum-throughput is decreasing.

In Fig.7, the sum-throughput of the cooperative schemes are almost unchanged relative to the rapid decline that of DT, which avails to improve system stability. However, due to the limition of the harvesting energy at all nodes, a continuous increase in the distance between S and R will cause the redution of the sum-throughput. By comparing the curves for different transmission protocols, we conclude that our proposed protocol significantly improves the sum-throughput in the case of RPL.

C. EFFECT OF SOURCE TRANSMIT POWER

Fig.8 shows the impact of the transmit power at S on the sum-throughput, where $d_0 = 20cm$ and $d_0 = 32cm$. It is observed that when P_S increases from $0.1mw$ to $1mw$, the optimal

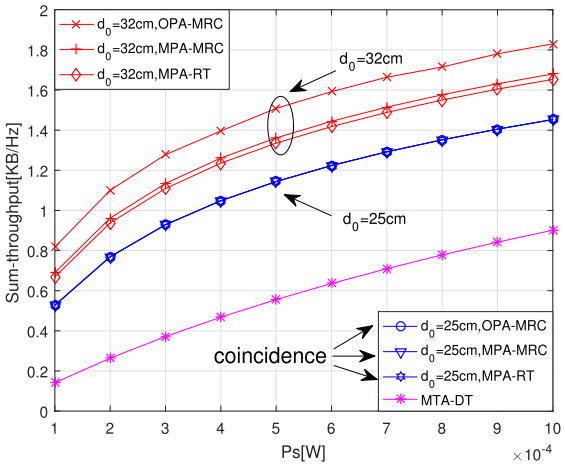

FIGURE 8. Optimal sum-throughput in different source power *Ps*.

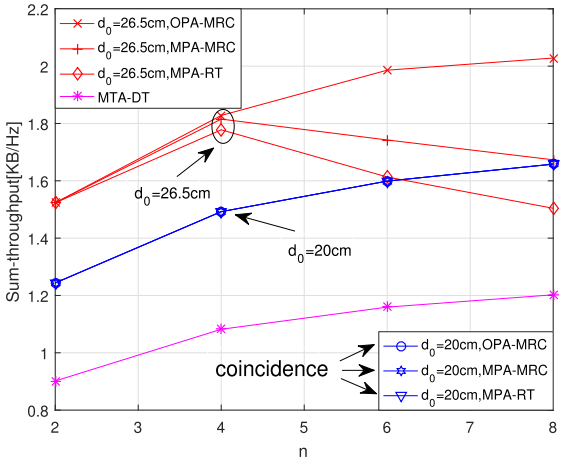

FIGURE 9. Optimal sum-throughput in different the number of destination nodes *n*.

throughput improves. This is intuitive, since increasing P_S improves the harvested energy at the relay and all destination nodes, which results in the relay transmit power and each destination node transmit power increase. We compare with the sum-throughput achievable by MPA-MRC, MPA-RT and MTA-DT, and our optimal strategy in sum-throughput is always better, respectively. Similar trends could be observed for the RPL case, which are not presented here due to space limitation.

D. EFFECT OF DESTINATION NODE NUMBER

Fig.9 plots the effect of destination nodes number on the sum-throughput with n from 2 to 8. It is assumed $d_0 = 20cm$ and $d_0 = 26.5cm$. The optimal sum-throughput based on OPA-MRC protocol and MTA-DT protocol is a increasing function of n. It is worth pointing out that the larger the number of destination node, the more slowly its amplitude increases, because the time assigned to D_i for information transmission decreases gradually. For MPA-RT protocol and MTA-DT protocol, the sum-throughput curves first goes up then drops when $d_0 = 26.5cm$; they gently rise when $d_0 = 20cm$. This is because that different relays harvest different energy. And the relay has more power near the soure, which ensures that the sum-throughput does not deteriorate with n increasing. Meanwhile, the sum-throughput on OPA-MRC outperforms the sum-throughput by MPA-MRC, MPA-DT and MTA-RT, respectively.

VI. CONCLUSION

In this paper, we have considered a OPA-MRC strategy for a cooperative WBAN in which the multiple destination nodes communicate with the source via a relay. The optimizatin problem is formed to maximize the sum-throughput, where the constraints are related to both the harvested energy at all destination nodes and the system maximum power. Moreover, it is analytically characterized by using the Lagrangian multiplier method. We analyze the effect of various system parameters, such as relay position, destination nodes positions, source power, and number of destination nodes in the two cases of OPA-MRC protocol. Our numerical results show that, despite of DPL case or RPL case, our optimal strategy can provide suerior performance campared to the conventional strategies. A remarkable sum-throughput improvement is achieved on the RPL case over the DPL case.

ACKNOWLEDGMENT

Part of this paper has been presented in 2019 IEEE/CIC International Conference on Communications in China (ICCC 2019).

APPENDIX A
PROOF OF LEMMA 2

For problem (P3), the objective function can be present as

$$F_1(\rho^d) = \frac{1}{2(1+n)} \sum_{i=1}^{n} \log_2 \left(1 + 2A(1+n)E_i^d \rho_i^d\right) \quad (33)$$

In (33), we assume $A = \frac{|g_i^{dr}|^2}{\sigma^2}$. By taking the second-order derivative of $F_1(\rho^d)$, we can obtain

$$\frac{\partial^2 F_1(\boldsymbol{\rho}^d)}{\partial^2 \rho_i^d} = -\frac{2(1+n)}{ln2} \frac{\left(AE_i^d\right)^2}{\left(1 + 2A(1+n)E_i^d \rho_i^d\right)^2} \quad (34)$$

Hence, the Hessian matrix of $F_1(\boldsymbol{\rho}^d)$ can be plotted by

$$H_1 = \nabla^2 F_1(\rho_1^d, ..., \rho_i^d, ..., \rho_n^d) = \begin{bmatrix} \frac{\partial^2 F_1(\boldsymbol{\rho}^d)}{\partial^2 \rho_1^d} & 0 & \cdots & 0 \\ 0 & \frac{\partial^2 F_1(\boldsymbol{\rho}^d)}{\partial^2 \rho_2^d} & \cdots & 0 \\ 0 & 0 & \cdots & \cdots \\ 0 & 0 & \cdots & \frac{\partial^2 F_1(\boldsymbol{\rho}^d)}{\partial^2 \rho_n^d} \end{bmatrix} \quad (35)$$

It is observed that all elements except that the main diagonal element are negative, other elements are zero. So, the Hessian matrix of $F_1(\boldsymbol{\rho}^d)$ is a negative definite matrix, then $F_1(\boldsymbol{\rho}^d)$ is convex [32].

APPENDIX B
PROOF OF LEMMA 3

For problem (P4), the objective function is given by

$$F_2(\boldsymbol{\rho}^r) = \frac{1}{2(1+n)} \sum_{i=1}^{n} \log_2\left(1 + 2B(1+n)\rho_i^r\right) \quad (36)$$

In (37), we assume $B = \left(\frac{E_i^d |g_i^{ds}|^2 J_i^{RPL} + E^r |g^{rs}|^2}{\sigma^2}\right)$. By taking the second-order derivative of $F(\boldsymbol{\rho}^d)$, we can obtain

$$\frac{\partial^2 F_2(\boldsymbol{\rho}^r)}{\partial^2 \rho_i^r} = -\frac{2(1+n)B^2}{ln2\left(1 + 2B(1+n)\rho_i^r\right)^2} \quad (37)$$

Thus, the Hessian matrix of $F_2(\boldsymbol{\rho}^r)$ can be written as

$$H_2 = \nabla^2 F_2(\rho_1^r, ..., \rho_i^r, ..., \rho_n^r) = \begin{bmatrix} \frac{\partial^2 F_2(\boldsymbol{\rho}^r)}{\partial^2 \rho_1^r} & 0 & \cdots & 0 \\ 0 & \frac{\partial^2 F_2(\boldsymbol{\rho}^r)}{\partial^2 \rho_2^r} & \cdots & 0 \\ 0 & 0 & \cdots & \cdots \\ 0 & 0 & \cdots & \frac{\partial^2 F_2(\boldsymbol{\rho}^r)}{\partial^2 \rho_n^r} \end{bmatrix} \quad (38)$$

Similarly, H_2 is also a negative definite matrix, which is exactly same to the case we considered in Appendix A. Hence, $F_2(\boldsymbol{\rho}^r)$ is convex [32].

REFERENCES

[1] U. Saarika, P. K. Sharma, and D. Sharma, "A roadmap to the realization of wireless body area networks: A review," in *Proc. Int. Conf. Elect., Electron., Optim. Techn. (ICEEOT)*, Mar. 2016, pp. 439–443.

[2] F. Hu, X. Liu, M. Shao, D. Sui, and L. Wang, "Wireless energy and information transfer in WBAN: An overview," *IEEE Netw.*, vol. 31, no. 3, pp. 90–96, May/Jun. 2017.

[3] Z. Wei, S. Gang, and C. Yong, "An improved WBAN route protocol based on DSR," in *Proc. IEEE Adv. Inf. Technol., Electron. Autom. Control Conf. (IAEAC)*, Dec. 2015, pp. 1142–1145.

[4] A. Rahim, N. Javaid, M. Aslam, Z. Rahman, U. Qasim, and Z. A. Khan, "A comprehensive survey of MAC protocols for wireless body area networks," in *Proc. 7th Int. Conf. Broadband, Wireless Comput., Commun. Appl.*, Nov. 2012, pp. 434–439.

[5] R. Chavez-Santiago, K. Sayrafian-Pour, A. Khaleghi, K. Takizawa, J. Wang, I. Balasingham, and H.-B. Li, "Propagation models for IEEE 802.15.6 standardization of implant communication in body area networks," *IEEE Commun. Mag.*, vol. 51, no. 8, pp. 80–87, Aug. 2013.

[6] D. Sui, F. Hu, W. Zhou, M. Shao, and M. Chen, "Relay selection for radio frequency energy-harvesting wireless body area network with buffer," *IEEE Internet Things J.*, vol. 5, no. 2, pp. 1100–1107, Apr. 2018.

[7] C. Yuen, M. Elkashlan, Y. Qian, T. Q. Duong, L. Shu, and F. Schmidt, "Energy harvesting communications: Part 2," *IEEE Commun. Mag.*, vol. 53, no. 6, pp. 54–55, Jun. 2015.

[8] R. Cavallari, F. Martelli, R. Rosini, C. Buratti, and R. Verdone, "A survey on wireless body area networks: Technologies and design challenges," *IEEE Commun. Surveys Tuts.*, vol. 16, no. 3, pp. 1635–1657, 3rd Quart., 2014.

[9] B. Han, R. Nielsen, C. Papadias, and R. Prasad, "Radio frequency energy harvesting for long lifetime wireless sensor networks," in *Proc. 16th Int. Symp. Wireless Pers. Multimedia Commun. (WPMC)*, Jun. 2013, pp. 1–5.

[10] D. Li and Y.-C. Liang, "Adaptive ambient backscatter communication systems with MRC," *IEEE Trans. Veh. Technol.*, vol. 67, no. 12, pp. 12352–12357, Dec. 2018.

[11] D. Li, W. Peng, and Y.-C. Liang, "Hybrid ambient backscatter communication systems with harvest-then-transmit protocols," *IEEE Access*, vol. 6, pp. 45288–45298, Sep. 2018.

[12] G. Yang, Q. Zhang, and Y.-C. Liang, "Cooperative ambient backscatter communications for green Internet-of-Things," *IEEE Internet Things J.*, vol. 5, no. 2, pp. 1116–1130, Apr. 2018.

[13] J. Gomez-Vilardebo, "Competitive design of power allocation strategies for energy harvesting wireless communication systems," in *Proc. IEEE Global Conf. Signal Inf. Process. (GlobalSIP)*, Dec. 2014, pp. 123–127.

[14] X. Zhou, R. Zhang, and C. K. Ho, "Wireless information and power transfer: Architecture design and rate-energy tradeoff," *IEEE Trans. Commun.*, vol. 61, no. 11, pp. 4754–4767, Nov. 2013.

[15] A. A. Nasir, X. Zhou, S. Durrani, and R. A. Kennedy, "Relaying protocols for wireless energy harvesting and information processing," *IEEE Trans. Wireless Commun.*, vol. 12, no. 7, pp. 3622–3636, Jul. 2013.

[16] L. Liu, R. Zhang, and K.-C. Chua, "Wireless information and power transfer: A dynamic power splitting approach," *IEEE Trans. Commun.*, vol. 61, no. 9, pp. 3990–4001, Sep. 2013.

[17] Q. Bu and J. Wang, "Performance analysis of video abstract delivery over cooperative wireless network in different fading channels," in *Proc. IEEE Symp. Comput. Appl. Commun.*, Jul. 2014, pp. 136–141.

[18] N. Qi, M. Xiao, T. A. Tsiftsis, L. Zhang, M. Skoglund, and H. Zhang, "Efficient coded cooperative networks with energy harvesting and transferring," *IEEE Trans. Wireless Commun.*, vol. 16, no. 10, pp. 6335–6349, Oct. 2017.

[19] S. Mahama, D. K. P. Asiedu, and K.-J. Lee, "Simultaneous wireless information and power transfer for cooperative relay networks with battery," *IEEE Access*, vol. 5, no. 7, pp. 13171–13178, 2017.

[20] A. Rahim and N. C. Karmakar, "Sensor cooperation in wireless body area network using network coding for sleep apnoea monitoring system," in *Proc. IEEE 8th Int. Conf. Intell. Sensors, Sensor Netw. Inf. Process.*, Apr. 2013, pp. 432–436.

[21] B. Lyu, D. T. Hoang, and Z. Yang, "User cooperation in wireless-powered backscatter communication networks," *IEEE Wireless Commun. Lett.*, vol. 8, no. 2, pp. 632–635, Apr. 2019.

[22] C. Han, B. Ai, L. Yang, and L. Liu, "DF-based cooperative spectrum sensing in multi-antenna cognitive radio network," in *Proc. 5th IET Int. Conf. Wireless, Mobile Multimedia Netw. (ICWMMN)*, Nov. 2013, pp. 145–149.

[23] H. Ju and R. Zhang, "Optimal resource allocation in full-duplex wireless-powered communication network," *IEEE Trans. Commun.*, vol. 62, no. 10, pp. 3528–3540, Oct. 2014.

[24] X. Kang, C. K. Ho, and S. Sun, "Full-duplex wireless-powered communication network with energy causality," *IEEE Trans. Wireless Commun.*, vol. 14, no. 10, pp. 5539–5551, Oct. 2015.

[25] S. Yin and Z. Qu, "Resource allocation in cooperative networks with wireless information and power transfer," *IEEE Trans. Veh. Technol.*, vol. 67, no. 1, pp. 718–733, Jan. 2018.

[26] Z. Ding, S. M. Perlaza, I. Esnaola, and H. V. Poor, "Power allocation strategies in energy harvesting wireless cooperative networks," *IEEE Trans. Wireless Commun.*, vol. 13, no. 2, pp. 846–860, Feb. 2014.

[27] H. Liu, F. Hu, S. Qu, Z. Li, and D. Li, "Multipoint wireless information and power transfer to maximize sum-throughput in WBAN with energy harvesting," *IEEE Internet Things J.*, vol. 6, no. 4, pp. 7069–7078, Aug. 2019. doi: 10.1109/JIOT.2019.2914147.

[28] D. Gunduz, K. Stamatiou, N. Michelusi, and M. Zorzi, "Designing intelligent energy harvesting communication systems," *IEEE Commun. Mag.*, vol. 52, no. 1, pp. 210–216, Jan. 2014.

[29] L. Wang, F. Hu, Z. Ling, and B. Wang, "Wireless information and power transfer to maximize information throughput in WBAN," *IEEE Internet Things J.*, vol. 4, no. 5, pp. 1663–1670, Oct. 2017.

[30] N. Zhao, F. Hu, Z. Li, and Y. Gao, "Simultaneous wireless information and power transfer strategies in relaying network with direct link to maximize throughput," *IEEE Trans. Veh. Technol.*, vol. 67, no. 9, pp. 8514–8524, Sep. 2018.

[31] E. Reusens, W. Joseph, G. Vermeeren, and L. Martens, "On-body measurements and characterization of wireless communication channel for arm and torso of human," in *Proc. 4th Int. Workshop Wearable Implant. Body Sensor Netw. (BSN)*, 2007, pp. 264–269.

[32] B. Sebastien, *Convex Optimization: Algorithms and Complexity*. Boston, MA, USA: Now, 2015, p. 1.

SHUANG LI received the B.S. degree from the College of Communication Engineering, Jilin University, Jilin, China, in 2017, where she is currently pursuing the M.S. degree with the Information and Signal Processing Laboratory. Her research interests include wireless power resource allocation and wireless body area networks.

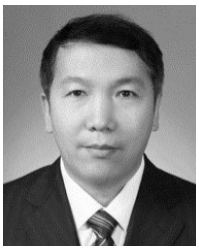

FENGYE HU received the B.S. degree from the Department of Precision Instrument, Xi'an University of Technology, China, in 1996, and the M.S. and Ph.D. degrees in communication and information systems from Jilin University, China, in 2000 and 2007, respectively, where he is currently a Full Professor with the College of Communication Engineering. He was a Visiting Scholar in electrical and electronic engineering with Nanyang Technological University (NTU), Singapore, in 2011. He has published 50 publications in IEEE journals and conferences. His current research interests include wireless body area networks, wireless energy and information transfer, energy harvesting, cognitive radio, and space-time communication. He is serving as an Executive Co-Chairs of IEEE/CIC International Conference on Communications in China (ICCC), China, in 2019. He is an Editor of *IET Communications*, *China Communications*, and *Physical Communication on Special Issue on Ultra-Reliable, Low-Latency and Low-Power Transmissions in the Era of Internet-of-Things*. He organized the first and second Asia-Pacific Workshop on Wireless Networking and Communications (APWNC 2013 and APWNC 2015). He also organized the Future 5G Forum on Wireless Communications and Networking Big Data (FWCN 2016).

ZHI MAO received the B.S. degree in communication engineering from the Changchun University of Science and Technology, Changchun, Jilin, China, in 2017. He is currently pursuing the Ph.D. degree in communication and information system with the Information and Signal Processing Lab, College of Communication Engineering, Jilin University, Changchun. His research interests include wireless body area networks, energy harvesting, multiple-input multiple-output, and cooperation communication.

ZHUANG LING received the B.S. degree from the College of Communication Engineering, Jilin University, Jilin, China, in 2016. He is currently pursuing the Ph.D. degree with the Information and Signal Processing Lab, College of Communication Engineering, Jilin University, Changchun, Jilin, China. His research interests include wireless body area networks, energy harvesting, and wireless networks.

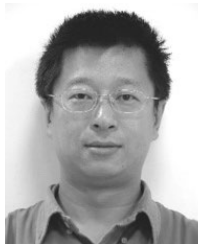

YONGKUI ZOU received the B.S. degree from the Department of Mathematics, Jilin University, China, in 1989, and the Ph.D. degrees from the Institute of Mathematics, Jilin University, in 1993, where he is currently a Full Professor with the School of Mathematics. He was a Visiting Scholar with Bielefeld University and University of Cologne in Germany, from 1994 to 1996, from 1998 to 2000, and from 2002 to 2003, respectively. His current research interests include numerical approximation of partial differential equations and stochastic differential equations.